Structure and magnetism of pulsed-laser-deposited ultrathin films of Fe on Cu(100)

H. Jenniches, J. Shen,* Ch. V. Mohan, S. Sundar Manoharan, J. Barthel, P. Ohresser, M. Klaua, and J. Kirschner
Max-Planck-Institut für Mikrostrukturphysik, Weinberg 2, D-06120 Halle/Saale, Germany
(Received 19 August 1998)

A layer-by-layer growth of ultrathin films right from the beginning would be desirable for establishing a straightforward correlation between magnetism and structure. We give experimental evidence that with the help of pulsed laser deposition (PLD) we can achieve layer-by-layer growth for Fe on Cu(100) in contrast to deposition by molecular-beam epitaxy. We present the results of a comprehensive study of the structural and magnetic properties of PLD-grown ultrathin Fe films of thicknesses between 2 and 10 monolayers (ML) deposited at room temperature. We show scanning tunneling microscopy images and low-energy electron-diffraction (LEED) patterns as well as intensity vs energy (IV) LEED curves demonstrating that PLD-grown Fe/Cu(100) has an isotropic fcc structure. We characterize the magnetic properties of our films by the magneto-optical Kerr effect. Following the improved growth and morphology, we found strong differences in the magnetic behavior of these films in comparison with Fe thermally deposited onto Cu(100): PLD-grown ultrathin Fe/Cu(100) shows an in-plane easy axis of magnetization in the thickness range 2–5 ML and again from about 10 ML, where the film structure is dominated by the bcc-Fe bulk phase, while there is a perpendicular easy axis of magnetization between 7 and 10 ML coverage. These results are discussed in terms of the different growth and structure due to the characteristic features of the PLD technique. [S0163-1829(99)13201-6]

I. INTRODUCTION

The deposition of Fe on Cu single crystals allows the room-temperature stabilization of γ-Fe, a fcc-Fe phase that promises interesting magnetic properties,[1] but usually only exists in bulk above 1186 K. The preparation and characterization of the Fe/Cu(100) system has attracted a lot of attention as a model system to investigate the correlation between magnetism and structure.[2–15] However, the thermal deposition (TD) of Fe/Cu(100) clearly exhibits a deviation from layer-by-layer growth in the first two monolayers (ML) as concluded from medium-energy electron-diffraction (MEED) studies.[2,3] This result has been confirmed by scanning tunneling microscopy (STM) investigations[4,5] in which the nucleation and growth of the second monolayer is observed to start from a total coverage of about 0.5 ML, which is long before the completion and even percolation of the first monolayer.[6] At thicknesses above 2 ML the growth appears to be layer by layer when characterized by MEED and STM, but more precise structural studies by low-energy electron diffraction (LEED) (Refs. 3 and 7–9) show that the growth of Fe/Cu(100) is much more complicated: It is divided into thickness ranges where different crystallographic structures are dominant, namely, tetragonally distorted fcc (fct), fcc, and bcc structures, where the latter is the equilibrium bulk phase of Fe at room temperature. In addition to that, superstructures have been observed which result from characteristic surface reconstructions and, furthermore, sinusoidal shifts of the atomic rows in plane and buckling out of plane have been proposed and confirmed by LEED crystallography.[9,10]

But as TD Fe/Cu(100) does not show straightforward layer-by-layer growth as would have been desirable for establishing a (more general) correlation between magnetism and structure for ultrathin magnetic films, it is difficult to link the measured magnetic properties to the complex structural transitions observed in this system. The Fe/Cu(100) system has appeared even more complicated due to the fact that both the structural and magnetic properties, in principle, also depend on the experimental conditions used, and although similar thermal deposition techniques were applied, reports seem to give contradictory information. The preparation of Fe/Cu(100) by a completely different deposition technique might lead to different magnetic behavior, and thus this work should contribute to the clarification of the correlation between structure and magnetism. On the background of the large number of publications on Fe/Cu(100), it is surprising that few attempts have been made[11] to systematically investigate the conditions under which Fe/Cu(100) shows the now established correlation between magnetic and structural properties.[10] So far, experiments to modify the structural properties of Fe/Cu(100) involved the annealing of the ultrathin films,[12] low-temperature growth,[13] or the use of surfactants during deposition.[14–16] The aim of this work is to find out whether and how the magnetic properties respond to a controlled growth manipulation without changing the temperature of the films or introducing surfactants into the films.

We recently found that we can modify the growth mode of Fe/Cu(100) from three-dimensional island to layer-by-layer growth from the initial stages of growth, if we use pulsed laser deposition (PLD) instead of a thermal deposition technique like electron beam evaporation.[17,18] In this contribution our objective is to prove that the growth of Fe/Cu(100) can also be modified with the help of PLD, in particular, in the initial stages (up to 2 ML). We present the results of a comprehensive study on PLD-grown Fe/Cu(100) of 2–10 ML thickness including STM and LEED investigations. We report the magnetic properties of our ultrathin films of Fe/Cu(100) in the 2–10 ML thickness regime, which is chosen mainly because the Curie temperature of the films is either too low (<2 ML) or too high (>10 ML) for the particular experimental setup of this work (140–450 K). The

results are discussed mainly on the background of the differences in the growth of Fe/Cu(100) as achieved with PLD.

PLD has been known for about three decades, but it only received major attention when it proved to be a most useful technique for the preparation of thin films of high-temperature superconductors about ten years ago.[19] The large number of publications[20,21] concerning the use of PLD makes it very clear that the main advantage of this technique is based on the fact that with the help of high-power lasers every possible material can be vaporized and, thus, deposited (in thin-film form) onto any substrate; i.e., PLD features congruent deposition (stoichiometry of the laser target is preserved in the film) of virtually any target material. Another very important advantage of PLD is the simplicity of the technique: The laser is completely decoupled from the actual deposition chamber—the laser beam is simply pointed onto a target inside the chamber through an appropriate viewport. Thus the preparation chamber can contain any working atmosphere.

The material deposition in PLD is achieved when the output of a short-time and high-power laser is focused onto a target, which, following the absorption of the light, results in a very rapid evaporation of the target material. Depending on the absorption, the evaporation takes place within a time of some nanoseconds. As there is no liquid phase for any longer period of time, there is not sufficient time for decomposition during the ablation process. If the laser pulse length is longer than the about 10 ns required for evaporation, significant absorption of the laser light occurs in the vapor emerging from the target. The absorption of light by the vapor results in the partial ionization of the evaporating atoms and, thus, in the formation of a plasma, which expands away from the target. This leads to the vaporized material to gain higher kinetic energies than in thermal deposition techniques. The expansion of the so-called plasma plume towards the target is blocked by the solid target, such that the plasma exerts a considerable recoil pressure onto the target surface, which, being heated before, causes an effect known as splashing, i.e., the emission of particulates and droplets from the target. There are other mechanisms which results in the formation of droplets mainly based on the macroscopic and microscopic patterning of the target due to the repeated impact of the high-power laser pulses.[22]

The emission of droplets and particulates is likely to be the reason why PLD has not really made an impact in the preparation of magnetic thin films. Typically, those particulates or droplets are of the order of microns in size and seriously limit the use of PLD for thin-film preparation depending on the specific application in mind[23] as most thin films have properties which are closely related to the quality of their ''two dimensionality,'' i.e., their continuous and homogeneous thickness and composition. However, there are a number of publications describing modifications to the experimental setup or the deposition parameters to considerably reduce or avoid droplet formation.[24–26] In our work, we choose to use low laser power (slightly above that of the ablation threshold) and work at a large target-substrate distance to avoid droplets.

Thin films of Fe have previously been grown by PLD.[27–32] However, in those publications thin films starting from several nanometers in thickness were prepared and studied. This work extends the previous research on Fe deposition by PLD into the range of ultrathin films, i.e., from submonolayer coverages to film thicknesses of some monolayers. We investigate PLD as a technique that is capable of modifying the growth mode and characterize the magnetic and structural properties of the film prepared in this way. Part of the results of our intensity vs energy (IV) LEED and magneto-optical Kerr effect (MOKE) studies has been recently published in brief.[33]

II. EXPERIMENTAL DETAILS

We have performed PLD in a multichamber ultrahigh-vacuum (UHV) system with a base pressure $\leqslant 5\times10^{-11}$ mbar and a pressure $\leqslant 2\times10^{-10}$ mbar during deposition. Prior to the evaporation, the Cu(100) substrate was subject to cycles of 1 keV Ar^+ sputtering and annealing at 870 K until clean Auger electron spectroscopy (AES) spectra, sharp LEED spots, and atomically smooth terraces under STM were obtained. In our multichamber system we also performed thermal deposition of Fe/Cu(100), and throughout the studies we regularly obtained results on TD samples to ensure that we can reproduce the results as published, for instance, in Refs. 2, 5, and 10. For the thermal deposition an Fe wire of 99.999% purity was heated by electron bombardment to deposit Fe at a rate of about 0.4 ML/min onto the Cu(100) crystal.

For PLD the output of an excimer laser with KrF (248 nm wavelength, 34 ns pulse length, maximum pulse energy 600 mJ, maximum repetition rate 30 Hz) was focused onto an Fe target of 99.99% purity, resulting in a fluence of about 5 J/cm^2 to deposition Fe onto the Cu(100) substrate, 100–130 mm away from the target. With the deposition parameters described, we have established conditions for the pulsed laser deposition of ultrathin films, for which we have not found any droplets on our samples. Using a pulse energy of 250–330 mJ and a repetition frequency of 5 Hz, we achieved an average deposition rate between 0.1 and 0.3 ML/min, which is comparable to the deposition rate during the thermal deposition.

Figure 1 shows a schematic of our PLD system. The deposition was monitored by a reflection high-energy electron-diffraction (RHEED) system using an electron beam of 35 keV incident onto the Cu(100) substrate under an angle of about 3° to have a relatively large distance between the specularly reflected and diffracted spots, whose intensities on a 4-in. phosphor screen were monitored using an automatic video-LEED system.[34] During deposition, the substrates were held at room temperature, i.e., 300 K$\pm$5 K. After deposition, the samples were transferred under UHV to a separate chamber dedicated to the magnetic characterization using both the polar and the longitudinal MOKE. The sample temperature during this measurement could be controlled from 140 to 450 K within $\pm$1 K. After the magnetic characterization samples were moved to an analysis chamber for LEED, intensity vs energy LEED measurements and AES for the investigation of the surface structure and the surface composition, and then to a room-temperature scanning tunneling microscopy chamber for topographic characterization.

III. RESULTS

A. Structural properties

MEED studies and STM investigations[2–8] on Fe/Cu(100) have shown that the thermal deposition of Fe/Cu(100) results

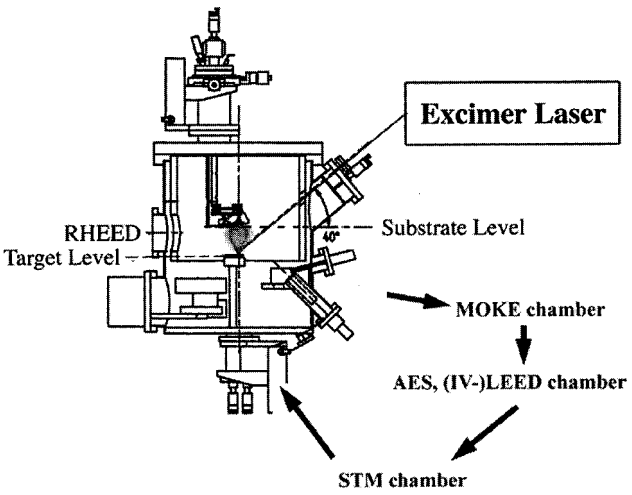

FIG. 1. Schematic of the pulsed laser deposition system with RHEED facilities and the typical characterization routine with the measurement of the magnetic (MOKE), structural (LEED and *IV*-LEED), and morphological (STM) properties within a multichamber UHV system.

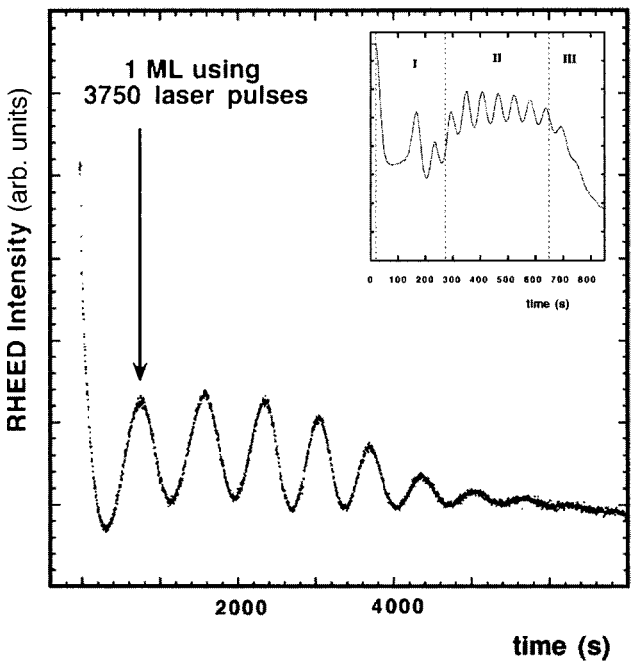

FIG. 2. RHEED oscillations of 10 ML pulsed-laser-deposited Fe/Cu(100) grown at room temperature showing very clear, regular oscillations, indicating that the growth proceeds via the layer-by-layer growth mode, *also* for the first 2 ML. The number of laser pulses required to deposit 1 ML of Fe is indicated. The average deposition rate during this experiment was 0.1 ML/min, which is at the slow end of the range of deposition rates available. Higher deposition rates can be achieved using a higher laser fluence, a higher repetition frequency, or a lower target-substrate distance. The inset shows irregular MEED oscillations as obtained during the thermal deposition of Fe/Cu(100) taken from our previous work (Ref. 15).

in a growth mode that is clearly not layer by layer in the first monolayers, while at thicknesses above 2 ML the growth appears to be layer by layer. Most researchers have found no MEED-RHEED oscillation for the first ML in the room-temperature growth of Fe/Cu(100).[2,15,35,36] Apparently, it is also possible to find a degraded or a considerably smaller than expected oscillation,[7,37] while one publication shows a full oscillation for the first ML.[38] In our thermal deposition of Fe/Cu(100) monitored with MEED, we have measured irregular oscillations as seen in Ref. 2 and our STM studies of the corresponding samples agree well with Refs. 4–6. However, in PLD of Fe/Cu(100) we have always recorded regular RHEED oscillations as shown in Fig. 2, from the initial stages to approximately 10 ML, above which the fcc-bcc transformation occurs. The regular oscillations are a strong indication that PLD growth of Fe/Cu(100) proceeds via the layer-by-layer growth mode, also for the first 2 ML. The amplitudes of the oscillations are decreasing after about 5 ML, but the growth mode remains layer by layer. For comparison, the inset in Fig. 2 shows irregular MEED oscillations as obtained during the thermal deposition of Fe/Cu(100) taken from our previous work.[15] The presence of oscillations in the intensity of electron-diffraction spots alone is no proof for a certain growth mode as, in principle, every slight variation in the crystal structure of the growing film could result in a change of the observed spot intensity. Complementary STM studies are, therefore, necessary for a conclusive characterization.

Room-temperature STM images have been taken after deposition, in support of the above claim that we can achieve true layer-by-layer growth of Fe/Cu(100) from the initial stages. In STM images topographic information of the STM tip, i.e., height, is translated into grey-scale pictures, where white corresponds to the highest height level and black to the lowest. In the study of the surface of an ultrathin film, the number of different successive atomic height levels ''visible'' is represented in a distribution of distinct grey levels, such that the number of different grey levels indicates the growth mode. Ideally, in layer-by-layer growth one should only see two grey levels within each substrate terrace: the substrate or underlying layer (dark) and the growing surface layer (bright). But typically there will be a third grey level, which is either due to the fact that the underlying layer is not yet filled completely or the nucleation of the next surface layer on top of a still growing layer owing to the fact that ideal layer-by-layer growth does not exist. By comparison with the height of atomic steps at the terrace edges of the clean and uncovered substrate, one can make sure that the islands on the surface are of monolayer height.

While the topography of our TD Fe/Cu(100) was in agreement with Refs. 4–6, PLD-grown Fe/Cu(100) is clearly exhibiting layer-by-layer growth from the initial stages as can be seen from Fig. 3. The inset in Fig. 3(c) shows a STM image of TD Fe/Cu(100) of a similar coverage to Fig. 3(c) on the same lateral scale, clearly displaying poor growth in the thermal deposition indicated by the significant coverage in the second monolayer at this thickness. For the PLD-grown Fe/Cu(100) it is evident that up to a coverage of 2 ML we observe a considerably improved growth compared to TD Fe/Cu(100) with random nucleation on the substrate terraces. For example, at the nominal thickness of 1 ML, more than 95% of the adatoms go to the first layer, while there is less than 5% in the second layer in PLD-grown Fe/Cu(100), contrary to the growth during thermal deposition where at 1 ML nominal coverage the first layer of the film is only 80% filled

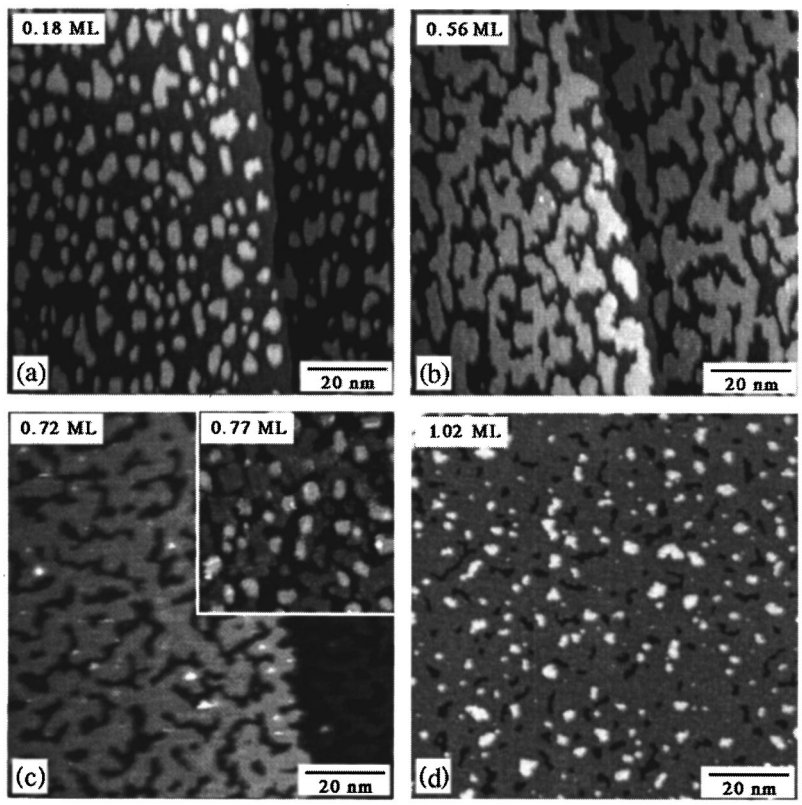

FIG. 3. STM images of the initial stages of growth of Fe/Cu(100) by pulsed laser deposition, clearly demonstrating layer-by-layer growth from the initial stages. There are less than 5% of both the substrate surface and second ML, visible in nominally 1-ML-thick pulsed-laser-deposited Fe/Cu(100). The inset in (c) shows part of a STM image of thermally deposited Fe/Cu(100) of a similar coverage than (c) on the same lateral scale, clearly displaying the poor growth in thermal deposition indicated by the significant coverage already present in the second ML at this thickness.

and nearly 20% are already in the second layer.[39] The growth of Fe/Cu(100) by PLD between 2 and 5 ML of thickness also proceeds via the layer-by-layer growth mode as is shown in Fig. 4; i.e., the growth in this thickness range compares well to the growth reported for TD Fe/Cu(100).[5] The sequence of STM images in Fig. 5 shows the topography of Fe/Cu(100) by PLD between 6 and 10 ML thickness, showing a general increase in the surface roughness and a faint indication of ''ridgelike'' structures[40] as are known from thermally deposited samples to be bcc precipitates. The bcc precipitates in fact start to appear at thickness of 4 ML with a very small density and become increasingly dominant when the thickness is higher than 7 ML. The bcc precipitates are elongated morphological features oriented along the $\langle 011 \rangle$ directions of the Cu(100) single-crystal substrate. Their orientation remains the same throughout the measurement in the thickness range from 4 to 10 ML, while the STM images were taken under various angles. The increasing number of ridges with increasing thickness is indicative of the transition from fcc to bcc and leads to an increased roughness of the film. Above 10 ML, the fcc to bcc transformation has been completed and the whole film becomes bcc-like.

This phase transformation is further evidenced in our LEED and *IV*-LEED studies. The comparison of the LEED patterns for 3.8 and 10.2 ML Fe/Cu(100) by PLD in Fig. 6 shows that the crystal structure has undergone a change with the thickness of the film. In the thickness range below approximately 9 ML, we always find only a sharp $p(1\times1)$ pattern with respect to the clean Cu substrate, indicating the true pseudomorphic growth of the Fe films. It should be noted at this point that we did not observe any of the superstructures resulting from surface reconstructions as frequently reported for TD Fe/Cu(100) in this thickness range $(4\times1, 5\times1, 2\times1)$.[2,7–10] However, the fcc-bcc phase transformation at around 10–11 ML thickness is clearly visible in the LEED patterns with its characteristic pseudo ''3×1'' superstructure resulting from the so-called Pitsch orientation at a similar thickness for TD Fe/Cu(100). The bcc-like structure is here leading to diffuse streaks into the $\langle 110 \rangle$ directions of the crystal in the LEED pattern. By performing thermal depositions of Fe on Cu(100) in the same multichamber UHV system, we confirmed that, in thermal deposition, superstructures were easily observed without any experimental difficulties.[41]

IV-LEED studies were undertaken to investigate the structural transitions in PLD-grown Fe/Cu(100) films and to supply some data comparable with the high-precision structure studies on TD Fe/Cu(100).[9–11] Figure 7 shows the (00) beam intensities vs energy [$I(E)$ or I-V] curves for films of different thicknesses. These curves were obtained at room temperature with the incident angle of the primary beam approximately 6° away from the surface normal with help of the automatic video-LEED system used to monitor the RHEED oscillations.[34] The *IV*-LEED curves look different to those recorded on TD Fe/Cu(100), although the same three peak families appear in the set of curves: peaks asso-

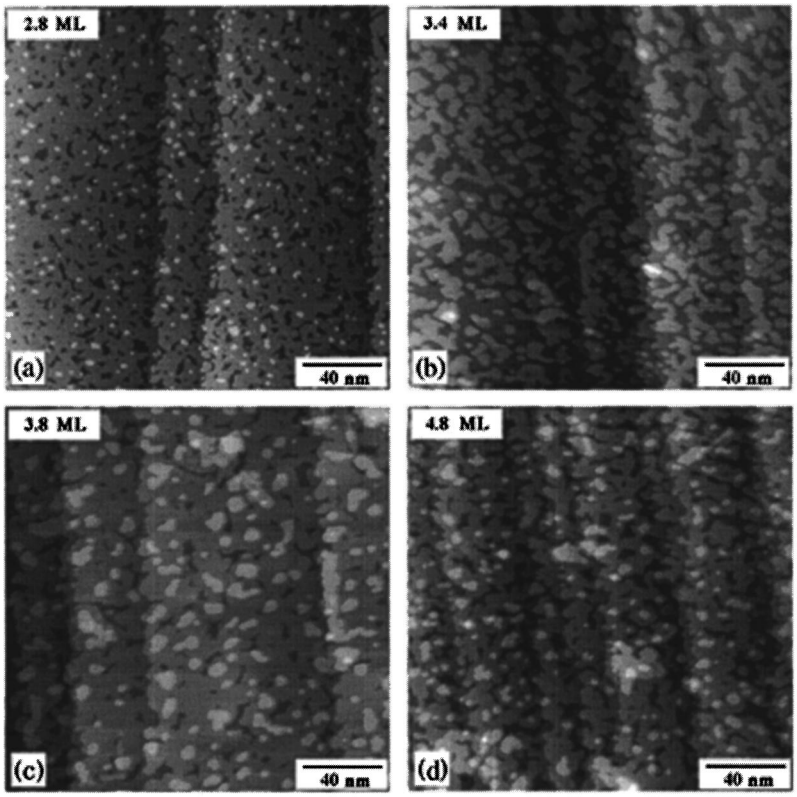

FIG. 4. STM images of 2–5-ML-thick Fe films on Cu(100) grown by pulsed laser deposition showing layer-by-layer growth, which compares well to the thermal deposition of Fe/Cu(100).

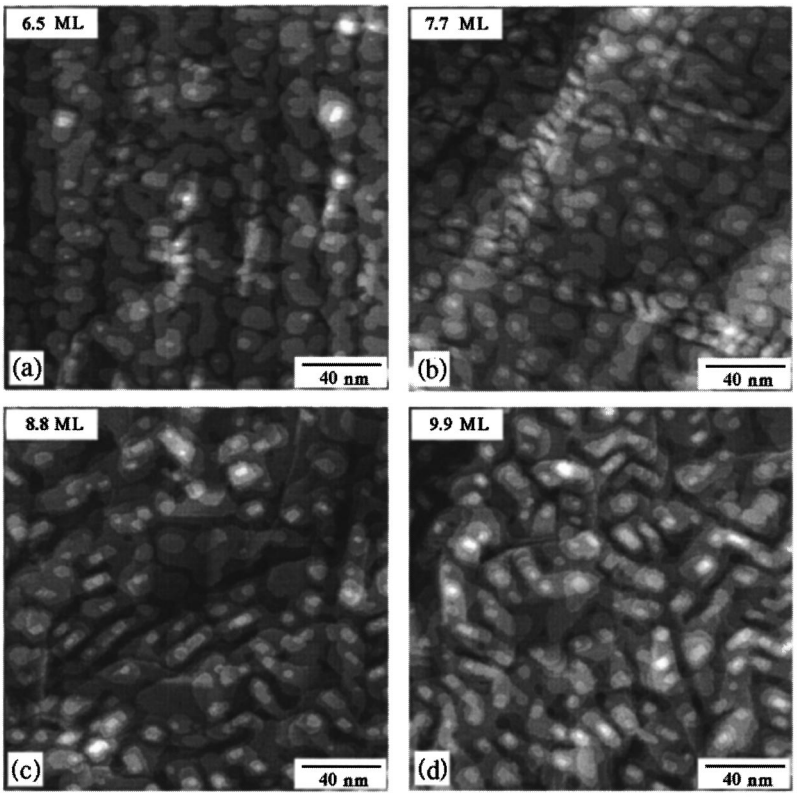

FIG. 5. STM images of 5–10 ML Fe/Cu(100) by pulsed laser deposition showing a general increase in the surface roughness and a faint indication of ''ridgelike'' structures (Ref. 40) as are known from thermally deposited samples to be precursors of the structural transformation from fcc to bcc, which seems to be completed above around 10 ML.

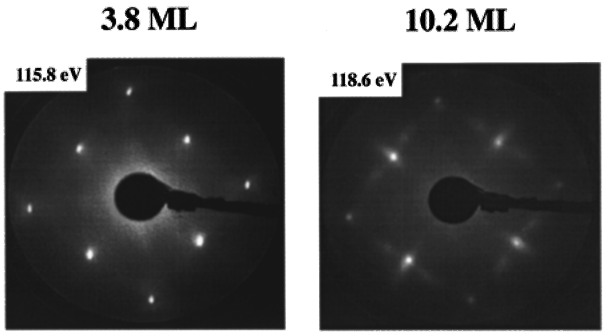

FIG. 6. LEED pattern of 3.8 ML Fe/Cu(100) on the left-hand side and 10.2 ML Fe/Cu(100) on the right-hand side, both prepared by pulsed laser deposition. The electron energy is indicated in the top left corner of each image. In the thickness range between 2 and 10 ML, we always find a sharp $p(1\times1)$ pattern with respect to the clean Cu substrate. At around 10–11 ML thickness the fcc-bcc phase transformation occurs, which is clearly visible in the LEED pattern of the 10.2-ML film showing a characteristic pseudo ''3 $\times1$'' superstructure.

ciated with the fcc structure, peaks related to the tetragonally distorted fct phase, and at the highest thickness (>10 ML) peaks representing the bcc bulk-Fe phase. The dashed lines in Fig. 7 mark the peak positions of the Cu substrate (fcc phase) and the solid lines follow the fct-Fe phase, which seems to be present in the low-energy range only, while the solid arrows show the bcc-Fe peaks only apparent at the highest thickness, indicating the completed transformation from the fcc into the bcc phase. A drastic difference compared to the *IV*-LEED curves obtained on TD Fe/Cu(100) is the fact that in PLD-grown Fe films there is no indication for the homogeneously distorted film structure (fct phase) reported for TD Fe/Cu(100) of thicknesses around 4 ML and below.[11] On the contrary, the fcc peaks are dominant throughout the thickness range investigated. We therefore believe that PLD-grown Fe films have an isotropic fcc structure; i.e., from the *IV*-LEED curves it seems that below a thickness of about 9 ML of Fe/Cu(100) there is no indication for a deviation of the structure from an fcc-phase Fe film with the possibility of a tetragonally distorted surface layer as seen in the *IV*-LEED curves by the fct peaks appearing only in the lower-energy range. In terms of the interlayer spacing, which can be deduced from the *IV*-LEED curves by simple kinematic approximation[42] there seems to be no significant variation of the fcc phase throughout the thickness range investigated as there is only a little shift of the peak positions with respect to the clean Cu(100) substrate peaks. In Fig. 8 we have plotted the ratio between the interlayer distances of the Fe film and Cu substrate, i.e., the c/a ratio, assuming the substrate Cu to be cubic and the Fe growth to be pseudomorphic, against the thickness of PLD-grown Fe/Cu(100). This relative value gives an indication for the distortion of the cubic structure. The c/a value is seen to increase up to a thickness of around 4 ML and then drops, reaching unity in the range between 5 and 7 ML, decreasing further below this value towards to ML. But throughout the thickness range from 2 to 10 ML, c/a only varies between 1.01 and 0.99. This is an indication of how close the structure of the PLD-grown films is to a cubic fcc lattice with the lattice constant of the Cu(100) substrate. Towards a thick-

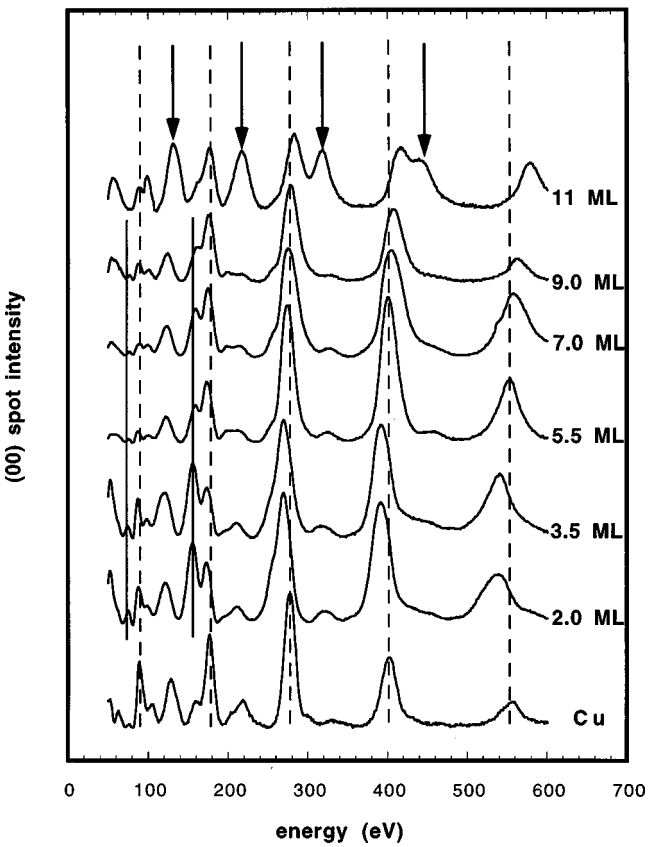

FIG. 7. IV-LEED curves recorded at room temperature for the (00) spot for various thicknesses of ultrathin films of Fe/Cu(100) grown by pulsed laser deposition (same coverage as in the STM images). The dashed lines mark the peak positions of the Cu(100) substrate (fcc phase), the solid lines follow the fct-Fe phase, which seems to appear in the low-energy range only, and the solid arrows show the bcc-Fe peaks, which indicate the transformation from the fcc into the bcc phase at a thickness above approximately 10 ML.

ness of 10 ML, there are increasing indications for a structural transformation; i.e., the *IV*-LEED curves show peak broadening and the formation of peak shoulders, but only in the *IV*-LEED curve for the Fe film about 10 ML does the

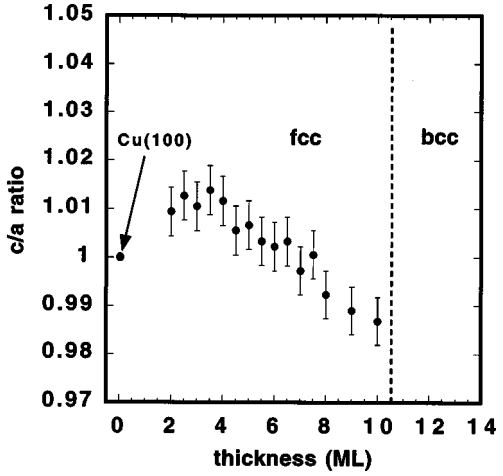

FIG. 8. Calculated c/a ratio of the PLD Fe/Cu(100) films as a function of thickness by kinematic method. In the whole thickness range, the c/a values are within 1% of unity.

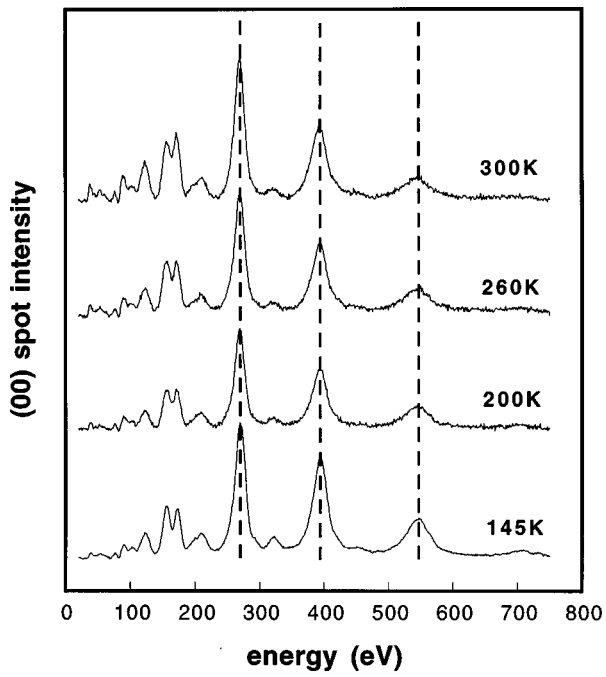

FIG. 9. Temperature-dependent *IV*-LEED curves measured from a 3-ML PLD Fe/Cu(100) film. Except for minor changes of the peaks at low energies, the main Bragg peak positions remain virtually unchanged.

transformation seem near to completion, as indicated by the pseudosuperstructure in the LEED pattern and the complete set of ''bcc'' peaks in the *IV*-LEED curves.[8]

It has to be noted that the absence of fct peaks in the *IV* curves of the PLD films is not affected by the measuring temperature. As an example, Fig. 9 shows the *IV*-LEED curves of a 3-ML PLD Fe/Cu(100) film measured at various temperatures ranging from 145 to 300 K. It is evident that except some minor changes of the low-energy peaks, the main Bragg peaks remain in the fcc position without showing signs of the appearance of fct peaks. The LEED pattern of the film also remains (1×1) without being affected by temperature. This implies that the fcc structure of the PLD-grown Fe films is rather stable, which is in great contrast to the TD Fe films whose structure is strongly affected by temperature.[11]

B. Magnetic properties

On the background of the established correlation between the structure and magnetism of the thermally grown Fe/Cu(100) films,[10] it is now even more interesting to investigate the magnetic behavior of the PLD Fe/Cu(100) films, as the ferromagnetic behavior of TD Fe/Cu(100) seems to be strongly connected to the presence of the fct phase,[11] which is absent in the PLD-grown Fe films. The magnetic behavior of PLD-grown Fe/Cu(100) turned out to look quite complicated, such that by just compiling hysteresis curves of samples with different thickness it seemed difficult to understand this behavior, especially in comparison with the results of the publications on TD Fe/Cu(100). We have, therefore, decided to plot the saturation magnetization (M_s) vs the thickness of the PLD-grown Fe films with exemplary polar and longitudinal Kerr hysteresis loops in the different thickness ranges, as seen in Fig. 10. The M_s in the plot was deduced from the saturation level measured from the polar Kerr hysteresis curves at 145 K, for which we have always obtained a well-defined saturation, except for samples of thicknesses above 10 ML, which are thought to be in the bcc structure. The M_s is seen to increase nearly linearly for PLD-grown Fe films in the thickness range up to 4 ML, just like it is observed for TD films. However, in thermally deposited films around 4 ML thickness, there is a strong decrease by about 75% to a low value of the magnetization, at which the magnetization remains virtually constantly low throughout the thickness range between 5 and 10 ML, which is explained by a ferromagnetic top layer, with the underlying layers being either paramagnetic[14] or antiferromagnetic.[38] In PLD-grown Fe/Cu(100) the M_s only drops by about 20% and then remains constant between 5 and 7 ML. It should be noted that the polar Kerr signal obtained from a fully saturated sample of about 7-ML PLD-grown Fe/Cu(100) was

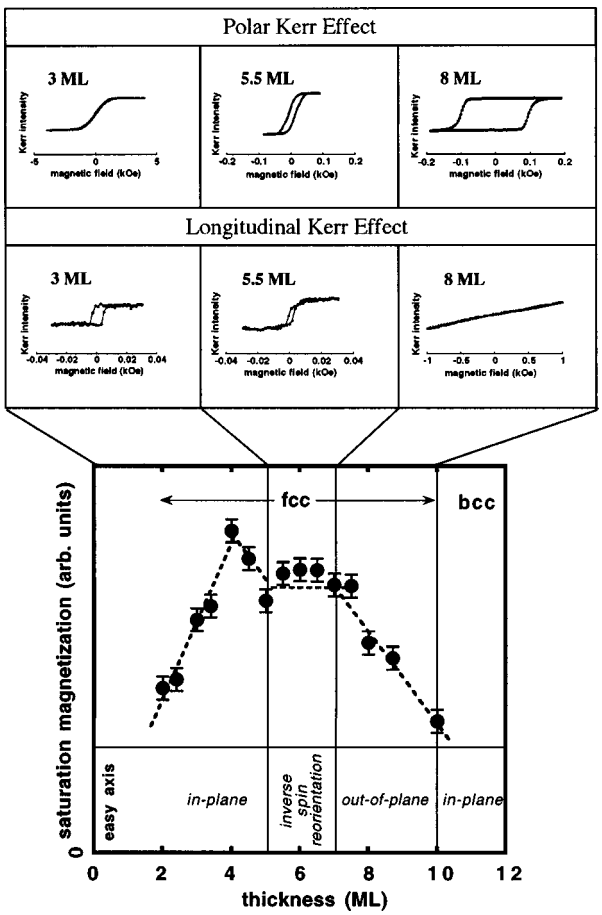

FIG. 10. Plot of the saturation magnetization vs thickness of Fe/Cu(100) grown by pulsed laser deposition indicating the magnetic phases. Exemplary MOKE curves in polar and longitudinal geometries both measured around 145 K are included to show hysteresis curves obtained on films from the three different characteristic thickness ranges, 2–5 ML (in-plane anisotropy), 5–7 ML (inverse spin reorientation region), and 7–10 ML (perpendicular anisotropy). Kerr loops of films from the bcc region are not shown, as their magnetic behavior is not fundamentally different from the known thermally deposited films. Note that the scales of the applied magnetic field for the Kerr loops are different and the units of the Kerr intensities are different for polar and in-plane geometry.

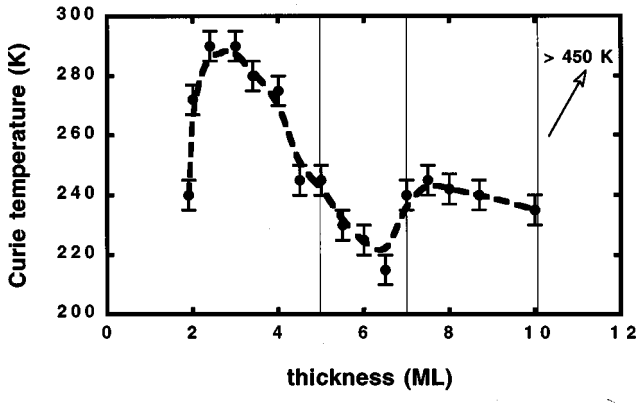

FIG. 11. Plot of the Curie temperature vs thickness of Fe/Cu(100) grown by pulsed laser deposition with an indication of the characteristic thickness ranges where different magnetic behavior is observed.

around a factor of 2 higher than the polar Kerr signal obtained from a comparably thick TD Fe film in our own experiments. By contrast, the polar Kerr signal at saturation of a 4-ML-thick PLD-grown sample was practically the same as the signal from a 4-ML thermally deposited Fe film. Above 7 ML, the M_s begins to decrease until it reaches a signal level similar to the 2-ML signal at a thickness of about 10 ML.

The magnetic anisotropy of the PLD Fe films shows rather complex behavior as shown in Fig. 10. The most outstanding feature is the fact that at thicknesses between 2 and 5 ML the easy axis of magnetization is in the plane of the film, while we can observe hard-axis loops in the polar Kerr-effect measurements, as can be seen in the Kerr loops in Fig. 10. However, the saturating field of these hard-axis perpendicular loops is relatively small with about 100 mT at 2 ML. The saturating field is then seen to decrease with increasing coverage, until at a thickness of around 5 ML significant remanent magnetization develops and, at higher thickness (7–10 ML), easy-axis (square) loops are observed out of plane. Above 10 ML, simultaneously with the development of the bcc phase, the easy axis of magnetization is rotating into the plane of the film; i.e., in-plane square hysteresis loops with a coercivity of around 400 Oe are observed.

Figure 11 shows a plot of the Curie temperature T_c vs the thickness of PLD-grown Fe/Cu(100). The maximum Curie temperature for PLD-grown films is reached at a lower thickness than the maximum in the saturation magnetization ($\sim$4 ML), which was also found for the TD films.[11] However, the T_c values for PLD-grown Fe/Cu(100) are, in general, lower than the ones for TD films. In particular, the maximum T_c at 3 ML is about 290 K for the PLD film and 370 K for the film prepared by thermal deposition. Above a thickness of 3 ML, the Curie temperature of PLD-grown Fe films drops to a minimum value of $T_c = 210$ K in the middle of the inverse spin reorientation region. Between 7 and 10 ML Fe/Cu(100) by PLD, T_c is nearly constant at around 240 K. Note that T_c for PLD-grown Fe/Cu(100) with a thickness of less than 10 ML is always below the deposition temperature of 300 K. Above this thickness range, in the bcc-Fe phase region, T_c is higher than 450 K. We did not perform temperature-dependent measurements above this temperature, in order to avoid any significant interdiffusion between the substrate and film material.

IV. DISCUSSION

As there is such a large number of publications on the thermal deposition of Fe/Cu(100), it seemed essential and unavoidable to discuss some of the results found on PLD-grown Fe/Cu(100) on the background of their comparison with the TD samples already in the results section of this paper. Here we will only shortly summarize the differences between PLD-grown and TD Fe/Cu(100) and then mainly discuss the implications of those differences.

(1) Morphology: By PLD, we have achieved true layer-by-layer growth in the first 2 ML of the growth of Fe/Cu(100).
(2) Structure: The crystal structure of the PLD-grown ultrathin Fe/Cu(100) films appears to be isotropic fcc Fe up to the thickness where the fcc-bcc transformation is completed at around 10 ML. The PLD-grown Fe films show no signs of surface reconstruction, but with indications that the surface layer is expanded with respect to the rest of the film.
(3) Magnetism: Between 2 and 5 ML thickness PLD-grown Fe/Cu(100) films have an in-plane easy magnetization axis. Between 5 and 7 ML the films experience an inverse spin reorientation from in plane to out of plane, resulting in a perpendicular easy magnetization axis in the thickness region between 7 and 10 ML. The M_s is linearly increasing up to a thickness of 4 ML and then drops by 20% and remains constant up to 7 ML, from where it slowly decreases.

A. Morphology

The STM images in combination with the RHEED oscillations during growth prove that ultrathin films of Fe on Cu(100) grown by PLD exhibit layer-by-layer growth, even in the initial states (below 2 ML), where the growth of TD Fe/Cu(100) films appears very poor. Layer-by-layer growth is a quality of growth and highly desirable as it allows the preparation of structurally well-defined films, where, for instance, magnetic properties are not disturbed by structural imperfections, as has been extensively discussed.[33,43] Layer-by-layer growth also implies a lower average surface roughness of the thin-film structure. PLD is known to lead to a better epitaxial growth.[20,21] In the present study experimental proof of the improved growth is given by sequences of STM images of submonolayer coverages and thicknesses of a few ML of a material deposited on a well-defined single-crystal substrate. The clear results of the STM studies are supported by RHEED oscillations, a surface structural characterization, and the presentation of magnetic properties, which are know to be ''notoriously structure sensitive.''[36] Recently, we demonstrated the applicability of PLD and improved growth preparing an artificially layered alloy, FeCu, by a stacking of monatomic layers of Fe and Cu onto a Cu(100) single crystal.[44]

We attribute the remarkable improvement in the growth to the fact that PLD features a very high deposition rate, the so-called ''instantaneous deposition:''[20] As the deposition rate in PLD is of the order of 0.001–0.01 ML per laser pulse and with the material deposition occurring within a time of the order of μs after each pulse, depending on the target-to-

substrate distance, the deposition rate during the pulse is in the range of 10^4 ML/s, which is six to seven orders of magnitude higher than in thermal deposition. This, however, means that we have a deposition technique in which one of the fundamental growth parameters, the deposition rate or flux of material F, is considerably higher than in conventional methods. Following scaling relationships, the island density N during nucleation and growth can be given by an expression of the form $N \sim (F/D)^{\gamma}$,[45] with D being the surface diffusion rate and γ being a parameter taking into account the size of the critical nucleus. Increasing F by six to seven orders of magnitude should lead to an increase in the density of nuclei or islands of around two orders of magnitude, assuming $\gamma = 0.33$; i.e., a dimer forms a stable nucleus on the surface. Thus, with an increased density of nuclei, ''normal'' surface diffusion is hindered, which inevitably results in two-dimensional growth. It has to be stressed that this kind of variation of a fundamental growth parameter is usually very difficult to achieve; for instance, the surface diffusion rate D is naturally distinctly limited by the temperature range available to the experiment. A large island density is evident from our STM images, showing many small features of monatomic height on the surface. However, in a quantitative evaluation of the island density during the initial stages of growth on Cu(100), it became clear that for room-temperature growth of Fe by PLD the island density is not decisively increased compared to TD Fe/Cu(100) as seen from our own[39] and other[4,6] STM investigations. But that might be due to the fact that the island density in the thermal deposition of Fe on Cu(100) is anomalously increased by the effective ''single-atom nucleation'' as reported in Ref. 46, where this effect is seen to be the reason for the poor growth in the initial stages observed by STM. It has to be pointed out that a critical nucleus of one atom does not really fit with the established scaling relationships,[45] although it is admitted that the size of the critical nucleus does not always seem to be well defined.[47] However, as we find layer-by-layer growth in the initial stages in PLD-grown Fe/Cu(100), we believe that the nucleation mechanism is modified with respect to the thermal growth mechanism. In fact, in the later stages of growth we still observe a large number of small islands of monatomic height in PLD, in contrast to the thermal deposition where the features generally become fairly large. A significant increase of the island density by around one order of magnitude in the initial stages of growth is readily found for the case of Fe/Cu(111) by PLD.[17,18] Thus we believe that ''instantaneous growth'' leads to layer-by-layer growth for the Fe/Cu(100) system. We recently found[17] that a certain control on the surface diffusion rate D is required by lowering the substrate temperature to less than 250 K during PLD, if true layer-by-layer growth should be achieved for systems like Fe/Cu(111) and Co/Cu(111), where thermal deposition results in the formation of three-dimensional islands due to the low surface energy, i.e., high surface diffusion rate. This is another proof that by using PLD we have a kind of control over fundamental growth parameters, which has not been available so far.

Some researchers claim that the influence of the high deposition rate is only secondary to the influence of the high particle energy for generating a better thin-film growth in PLD.[20,48] In thermal evaporation techniques like electron-beam evaporation or evaporation from a Knudsen cell, the ''evaporating'' atoms have thermal kinetic energies ($\ll 1$ eV). In PLD there is a certain distribution of different kinetic energies, which highly depends on the laser wavelength, the target material, and, in particular, the fluence used. We are operating our PLD system in a fluence region just above the so-called ablation threshold under which no significant evaporation from the target material occurs; i.e., we are using deposition rates which are very low for PLD systems. The average deposition rate during PLD is still of the same order of magnitude as in thermal deposition. With the experimental setup and conditions we use, we are working in a regime which is known to produce only a small amount of ions with higher kinetic energies and a large number of neutral atoms with average kinetic energies of the order of a few eV.[49] Kinetic energies of a few eV are certainly not changing the growth compared to energies of $\ll 1$ eV due to the energy gain on adsorption of an atom, which remains of the order of several eV in both cases. It is nevertheless conceivable that a small higher-kinetic-energy ion pulse during PLD could further improve the growth as has been observed in some homoepitaxial systems[50] and recently in a heteroepitaxial system.[51] We have, however, not observed any damage to the single-crystal surface or indications that islands are pinned to a certain position, as could be assumed for the presence of high-kinetic-energy ions.

We also do not seem to have the droplet problem. The field of view in the STM is limited, and the deposition of droplets is a statistical process, such that there should be a probability of a few percent to encounter a problem during the STM investigation of a film of around 10 ML thickness (assuming droplet densities as found in Ref. 29). However, we believe that the above deposition parameters are also optimized to avoid droplet formation, as we have not observed any such features during the study of literally several thousands of STM images. Even using scanning electron microscopy we did not observe any droplets. Another indication for the absence of the droplet problem comes from the fact that we have not detected any degradation of the various single-crystal substrates used during the course of this investigation, given the fact that our sputter cleaning is optimized for the deposited layer thickness and not for removing any larger scale features. Considering that both droplets and an increasing number of atoms and ions with higher kinetic energy are emitted from the laser target once the fluence increases further above the ablation threshold, we recommend to work as close to the threshold as possible, giving away the advantage that the average deposition rate could otherwise be even higher, for instance, of the order of nm/s. For the preparation of ultrathin films by PLD, it is also essential to work under true UHV conditions and with a large target-substrate distance.

B. Structure

The most notable result from our structural analysis lies in the fact that the LEED measurements indicate that from 2 to 10 ML the inner layers of the PLD-grown Fe/Cu(100) films have a structure which is very close to cubic fcc. This is backed by the fact that the PLD films exhibit (1×1) structure in the lateral direction, as well as the fact that there is hardly tetragonal distortion in the vertical direction accord-

ing to our kinematic *IV*-LEED calculation. In principle, the kinematic calculation does not normally allow a quantitative interpretation claiming an accuracy in the percentage region of the structural parameters. However, in this particular system Fe/Cu(100), we believe that the kinematic calculation is justified for the following reasons.

(1) In previous work, the structure of the Fe/Cu(100) system has been extensively studied including using the state-of-the-art full dynamical calculation.[52] A detailed comparison between the kinematic and dynamic calculations regarding this system has also been made, which indicate that a kinematic analysis of the Bragg peak positions provides reliable ways to separate the fcc and fct phases in the films. It turned out that even the quantitative analysis within its limits agreed well with the full dynamic analysis. The reason is probably that Fe/Cu(100) displays largely kinematical Bragg peaks for near-normal incidence at energies above 100 eV.

(2) In the PLD films there is only one family of peaks (at high energies) which have close energy positions to those of the substrate copper peaks, i.e., fcc peaks. In addition, there are no signs of atomic buckling (at least in the lateral direction). Therefore, in our kinematic calculation of the PLD films, we are not involved in complex problems such as distinguishing the fct from the buckling, which can only be done and has been successfully done by dynamic calculations for TD films.[51]

While the inner layers of the PLD films remain cubic-like throughout the whole thickness region (2–10 ML), there are also indications showing that the topmost layers of the PLD films are somewhat expanded with respect to the average interlayer distances of the Cu single-crystal substrate. In this respect the PLD films seem to assemble the structure of the TD Fe/Cu(100) films above 5 ML, where the films were observed to have an expanded topmost layer and cubic inner layers. However, we have observed no superstructure in the topmost layers of the PLD films, while the top layers of the TD films (>5 ML) are (2×1) reconstructed. Moreover, even the lateral lattice constant of the innerlayers of the PLD and TD films may be different due to the different extent of the ongoing fcc-bcc phase transformation. Since the bcc structure has a larger lattice, it is expected that the transformed bcc precipitates will accommodate partially the strain in the epitaxial films. Such a strain accommodation will in turn influence the lattice constant of the untransformed fcc parts. This appears to be particularly important to understand the surprising difference between the magnetic properties of the PLD and TD films, as will be discussed in the next section.

For films below 5 ML, as stated above, the PLD films have a fcc structure, while the TD films have a fct structure. Based on previous theoretical calculations,[1] it is often assumed that fcc Fe should have a slightly larger lattice constant than Cu in order to possess the high-spin ferromagnetic state. The fact that the TD Fe/Cu(100) films (<5 ML) have a fct structure, i.e., a larger atomic volume than that of the copper, has been considered as direct proof of the calculation. However, our results from the PLD films have clearly indicated that the Fe/Cu(100) films can be high-spin ferromagnetic when the films adopt the lattice constants of the copper substrate in both directions. It is not immediately clear which structure stands for a more stable state of the Fe/Cu(100). By the fact that the fct structure of the TD Fe films is unstable against temperature,[53] while the fcc structure of the PLD films is stable against temperature (Fig. 9), one may conclude that the fcc structure is at least more stable with respect to temperature changing. It remains unclear, however, whether the fcc structure of the PLD films is a direct consequence of the accomplishment of layer-by-layer growth from the initial states in PLD Fe/Cu(100), as this would raise the question of whether in turn the distorted and surface-reconstructed structures observed in the TD films are due to the poor islandic nucleation and the clear deviation from layer-by-layer growth in the initial stages.

C. Magnetism

The different magnetic behavior between the TD and PLD films reflects the complex and rich magnetic structures of fcc Fe. The initial linear increase of M_s suggests that the films have a ferromagnetic phase below 4 ML. The measured Kerr intensities of the PLD and TD Fe films are practically the same, indicating that the PLD fcc-like films (<4 ML) have also a high-spin ferromagnetic phase. The decrease of M_s above 4 ML is an indication that the Fe films are either nonuniformly magnetized or possess a smaller magnetic moment. The latter can be ruled out because M_s, instead of being constant or even decreasing as shown in Fig. 10, should increase with increasing thickness, though with a smaller slope than the high-spin one (<4 ML). A recent theoretical calculation[54] has demonstrated a large amount of possible antiferromagnetic-(AFM) type spin configurations of the Fe/Cu(100) films at higher thickness (>4 ML), with the most stable configuration being a bilayer-antiferromagnetic state at even layers (6 ML) and a coexistence of several spin states, for instance, two spin-up on top of three spin-down layers, at odd layer numbers (5 ML). But the suggested AFM structure would result in a considerably smaller net magnetization than the experimental values between 5 and 7 ML, and is particularly inconsistent with the fact that the M_s continuously decreases with increasing thickness from 7 to 10 ML. Other collinear spin alignment calculations[55] also propose antiferromagnetic spin configurations which yield smaller values for the magnetization than the ones we measured.

In the following we raise a plausible argument for the inconsistency between theory and experiment. While the theories[54,55] assume an unchanged fcc structure for all film thickness, the lattice constant of the experiment films may be changed by increasing thickness, because above 4 ML the films start to experience a fcc to bcc structural transformation. The transformed bcc precipitates have a larger lattice constant and tend to partially accommodate the strain in the films. As a result, a portion of the inner layers of the films may relax to bulklike fcc (possibly with a lattice constant similar to that of the fcc Fe precipitates in a Cu matrix), i.e., nonpseudormorphic, which is known to be nonmagnetic above the Néel temperature (67 K in the case of bulk). The topmost layers, however, should remain ferromagnetic due to the vertical expansion. Because the fcc to bcc transformation initially proceeds very slowly, the portion of the nonpseudormorphic part of the inner layers of the Fe films varies little,

explaining the rather constant M_s between 5 and 7 ML. At higher thickness the transformation proceeds rapidly, leading to a larger and larger portion of the nonpseudormorphic inner layers of the Fe films. This explains why the M_s of the films decreases with increasing thickness from 7 to 10 ML. At 10 ML the topmost layers appear to be the only ferromagnetic layers, since the M_s equals nearly that a 2-ML film. It is not clear whether the transformed bcc precipitates are magnetic or not, but they do not contribute to the measured M_s because our applied magnetic field is not large enough to saturate bcc films (>5 ML) in the perpendicular direction.

A similar mechanism can be used to solve the puzzle as to why the fcc-like PLD films (<4 ML) have a high-moment ferromagnetic phase while the fcc-like TD films (5–11 ML) are antiferromagnetic. According to our STM studies, the PLD films (<4 ML) are free of bcc structures, while the TD films (5–11 ML) contain bcc precipitates which tend to accommodate the strain in the film. Thus part of the TD films (5–11 ML) should relax to have bulk lateral lattice (room temperature fcc Fe lattice extrapolated from high-temperature values), i.e., nonpseudormorphic. Because full dynamic LEED calculations indicated that the topmost layers are still fct-like and thus strained, it is likely that the fcc-like inner layers are actually nonpseudormorphic. The PLD films (<4 ML), on the other hand, should adopt the lateral lattice constant of copper, which is slightly larger than that of bulk fcc Fe. Under these assumptions, it is straightforward to understand that the TD films (5–11 ML) have an antiferromagnetic phase which is similar to the bulk fcc Fe, while our studies indicate that the pseudormorphic fcc Fe/Cu(100) has a high-moment ferromagnetic phase.

It is somewhat astonishing that we have observed an in-plane easy axis of magnetization in PLD-grown Fe/Cu(100) between 2 and 5 ML thickness, while the TD films exhibit perpendicular magnetic anisotropy in this thickness range. Regarding the in-plane easy axis in the PLD-grown Fe/Cu(100), we already pointed out that contrary to the typical uniaxial anisotropy we have indications that this is not a very strong in-plane anisotropy as the samples can be saturated quite easily in moderate magnetic fields in the out-of-plane geometry. Thus there seems only to be a weak perpendicular anisotropy, which in turn allows the shape anisotropy to become dominant, such that the easy axis of magnetization is in plane. Theoretically, it remains a matter of dispute whether the positive surface anisotropy is large enough to overcome the shape anisotropy in the Fe/Cu(100) system. Ujfalussy *et al.*[56] have found that for ferromagnetic (FM) Fe films, the surface anisotropy is too small to overcome the shape anisotropy at any thickness. This is consistent with the measured in-plane magnetization below 5 ML (Fig. 2), where the films are in a FM state. Results by Lorentz and Hafner,[55] however, predict perpendicular magnetization for FM Fe films. It has to be pointed out at this stage of the discussion that for reasons of simplicity most calculations of the magnetic properties and the anisotropy of Fe/Cu(100) have assumed a perfect isotropic cubic unit cell and perfectly smooth films,[54–56] which are not found in TD Fe/Cu(100) of thicknesses below 4 ML. There have hardly been attempts to take the tetragonal distortion of the unit cell into account, not to mention the totally reconstructed film structure below 4 ML or the buckling out of plane in combination with sinusoidal shifts in the atomic structure, as deduced from the high-precision LEED investigations.[9,10,52] Some researchers claim[57,58] that the perpendicular magnetic anisotropy, which is found in TD Fe/Cu(100), is only due to the tetragonally expanded fct structure, and is partially attributed to the volume of the unit cell and partially also to the anisotropy of the structure, as the lattice is vertically expanded. Thus, if this support from the crystal structure is not present, the competition of the anisotropies will be differently balanced and the surface anisotropy might well not be the dominant part. Experimental evidence for this seems to come from extended x-ray-absorption fine-structure (EXAFS) studies of Cu-Fe-Cu sandwich structures,[57] where the distortion of the Fe film is completely removed and an isotropic fcc structure is obtained by coating the Fe film with Cu. The perpendicularly distorted crystal structure is also not found to play a major role in the structure of PLD-grown Fe/Cu(100) following our LEED and *IV*-LEED results. Thus the easy axis of magnetization could be in plane in the range between 2 and 4 ML of Fe/Cu(100) by PLD, as the structure is isotropic fcc and the film is in its ferromagnetic state due to its reduced dimensionality, as explained above. Another contribution might come from the morphology of the films. We have observed layer-by-layer growth in Fe/Cu(100) by PLD and ascribe this to the high deposition rate which is forcing two-dimensional growth due to the formation of an increased number of monatomically high islands. There are calculations[59] which predict the change of the direction of the magnetic moments around step edges with particular emphasis on the case where the surface has step edges, for instance, between the fifth layer and the fourth layer coverage in TD Fe/Cu(100), where the transformation from the uniform ferromagnetic to the antiferromagnetic spin configuration occurs. In an evaluation of monolayer-scale surface roughness Bruno,[60] estimated a reduced anisotropy around step edges. In a film with a high density of monolayer high islands, we have an increased number of step edges, which for either of the above calculations could lead to a reduced surface anisotropy and, thus, be responsible for the appearance of an in-plane easy axis of magnetization.

The reason why the PLD films become perpendicularly magnetized at higher thickness (7–10 ML) is not clear. It may be associated with magnetic phase transitions, as in this thickness region the films become mainly nonmagnetic or antiferromagnetic depending on the temperature. Since both calculations of Refs. 55 and 56 consistently predict a perpendicular magnetization for thicker Fe/Cu(100) films which have an antiferromagnetic ground state, at this stage we tentatively attribute the spin reorientation to the ferromagnetic to antiferromagnetic phase transformation.

V. CONCLUSION

Using PLD, we have achieved layer-by-layer growth of Fe/Cu(100) from the initial stages. This improvement in the growth is due to a characteristic feature of PLD, the very high deposition rate. The growth above a thickness of 2 ML seems comparable to the growth of TD samples; i.e., it proceeds layer by layer. However, the crystal structure of the inner layers of the PLD-grown ultrathin Fe/Cu(100) films appears to be isotropic fcc Fe up to 10 ML above which the fcc-bcc transformation is completed.

The magnetic behavior of PLD-grown Fe/Cu(100) is quite different from TD samples: Below a thickness of about 5 ML, the Fe films show an easy axis of magnetization in the film plane. Then the films undergo an inverse spin reorientation from in plane to out of plane, such that there is a perpendicular easy axis of magnetization between 6 and 10 ML. At a thickness above approximately 10 ML, a reorientation of the easy axis of magnetization occurs back into the plane of the film, which is associated with the fcc-bcc transformation being completed.

With PLD we seem to have an ideal technique to easily modify the growth and structure of ultrathin films. The correlation between structure and magnetism characterized by the magnetic anisotropy eventually allows us in this way to manipulate the magnetic properties of ultrathin films.

ACKNOWLEDGMENTS

The authors are grateful to F. Pabisch and G. Kroder for their technical assistance.

*Author to whom correspondence should be addressed. Present address: Solid State Division, Oak Ridge National Lab., Oak Ridge, TN 37831-6057.

[1] V. L. Moruzzi, P. M. Marcus, and J. Kübler, Phys. Rev. B **39**, 6957 (1989).
[2] J. Thomassen, B. Feldmann, and M. Wuttig, Surf. Sci. **264**, 406 (1992).
[3] M. Wuttig and J. Thomassen, Surf. Sci. **282**, 237 (1993).
[4] D. D. Chambliss, K. E. Johnson, R. J. Wilson, and S. Chiang, J. Magn. Magn. Mater. **121**, 1 (1993).
[5] J. Giergiel, J. Shen, J. Woltersdorf, A. Kirilyuk, and J. Kirschner, Phys. Rev. B **52**, 8528 (1995).
[6] D. D. Chambliss and K. E. Johnson, Surf. Sci. **313**, 215 (1994).
[7] H. Landskron, G. Schmid, K. Heinz, K. Müller, C. Stuhlmann, U. Beckers, M. Wuttig, and H. Ibach, Surf. Sci. **256**, 115 (1991).
[8] M. Wuttig, B. Feldmann, J. Thomassen, F. May, H. Zillgen, A. Brodde, and H. Neddermeyer, Surf. Sci. **291**, 5 (1993).
[9] S. Müller, P. Bayer, C. Reischl, K. Heinz, B. Feldmann, H. Zillgen, and M. Wuttig, Phys. Rev. Lett. **74**, 765 (1995).
[10] K. Heinz, S. Müller, and P. Bayer, Surf. Sci. **352–354**, 942 (1996).
[11] M. Zharnikov, A. Dittschar, W. Kuch, C. M. Schneider, and J. Kirschner, Phys. Rev. Lett. **76**, 4620 (1996).
[12] J. Shen, J. Giergiel, A. K. Schmid, and J. Kirschner, Surf. Sci. **328**, 32 (1995).
[13] R. Allenspach and A. Bischof, Phys. Rev. Lett. **69**, 3385 (1992).
[14] J. Thomassen, F. May, B. Feldmann, M. Wuttig, and H. Ibach, Phys. Rev. Lett. **69**, 3831 (1992).
[15] A. Kirilyuk, J. Giergiel, J. Shen, M. Straub, and J. Kirschner, Phys. Rev. B **54**, 1050 (1996).
[16] Dongqi Li, M. Freitag, J. Pearson, Z. Q. Qiu, and S. D. Bader, J. Appl. Phys. **76**, 6425 (1994).
[17] H. Jenniches, M. Klaua, H. Höche, and J. Kirschner, Appl. Phys. Lett. **69**, 3339 (1996).
[18] J. Shen, P. Ohresser, Ch. V. Mohan, M. Klaua, J. Barthel, and J. Kirschner, Phys. Rev. Lett. **80**, 1980 (1998).
[19] D. Dijkamp, T. Venkatesan, X. D. Wu, S. A. Shaheen, N. Jisrawi, Y. H. Min-Lee, W. L. McLean, and M. Croft, Appl. Phys. Lett. **51**, 619 (1987).
[20] J. T. Cheung and H. Sankur, CRC Crit. Rev. Solid State Mater. Sci. **15**, 63 (1988).
[21] See, e.g., *Pulsed Laser Deposition of Thin Films*, edited by D. B. Chrisey and G. K. Hueber (Wiley, New York, 1994).
[22] S. Fähler, M. Strömer, and H. U. Krebs, Appl. Surf. Sci. **109/110**, 433 (1997).
[23] J. C. S. Kools, in *Pulsed Laser Deposition of Thin Films* (Ref. 21), Chap. 19.
[24] J. P. Gavigan, in *Science and Technology of Nanostructured Magnetic Materials*, edited by G. C. Hadjipanayis and G. A. Prinz (Plenum, New York, 1991).
[25] A. A. Gorbunov, W. Pompe, A. Sewing, S. V. Gaponov, A. D. Akhsakhalyan, I. G. Zabrodin, I. A. Kas'kov, E. B. Klyenkov, A. P. Morozov, N. N. Salaschenko, R. Dietsch, H. Mai, and S. Völlmar, Appl. Surf. Sci. **96–98**, 649 (1996).
[26] B. Holzapfel, B. Roas, L. Schultz, P. Bauer, and G. Saeman-Ischenko, Appl. Phys. Lett. **61**, 3178 (1992).
[27] Yu. A. Bykovski, V. M. Boyokov, V. T. Galochkin, A. S. Molchanov, I. N. Nokolaev, and A. N. Orevskii, Sov. Phys. Tech. Phys. **23**, 578 (1978).
[28] S. Keitoku and H. Ezumi, IEEE Transl. J. Magn. Jpn. **7**, 858 (1992).
[29] J. C. S. Kools, R. Coehoorn, F. J. G. Hakkens, and R. H. J. Fastenau, J. Magn. Magn. Mater. **121**, 83 (1993).
[30] N. Cerief, D. Givord, O. McGrath, Y. Otani, and F. Robaut, J. Magn. Magn. Mater. **126**, 225 (1993).
[31] H. U. Krebs and O. Bremert, in *Laser Ablation in Materials Processing: Fundamentals and Applications*, edited by B. Braren, J. Dubowski, and D. Norton, MRS Symposia Proceedings No. 285 (Materials Research Society, Pittsburgh, 1993), p. 527.
[32] D. Cole, R. Jordan, J. G. Lunney, and J. M. D. Coey, J. Magn. Magn. Mater. **165**, 246 (1997).
[33] J. Shen, H. Jenniches, Ch. V. Mohan, J. Barthel, M. Klaua, P. Ohresser, and J. Kirschner, Europhys. Lett. **43**, 349 (1998).
[34] J. Giergiel, H. Hopster, J. M. Lawrence, J. C. Hemminger, and J. Kirschner, Rev. Sci. Instrum. **66**, 3475 (1995).
[35] D. A. Steigerwald and W. F. Egelhoff, Jr., Surf. Sci. **192**, L887 (1987).
[36] A. Schatz, S. Dunkhorst, S. Lingnau, U. v. Hörsten, and W. Keune, Surf. Sci. **310**, L595 (1994).
[37] A. Kirilyuk, J. Giergiel, J. Shen, and J. Kirschner, Phys. Rev. B **52**, R11 672 (1995).
[38] Dongqi Li, M. Freitag, J. Pearson, Z. Q. Qiu, and S. D. Bader, Phys. Rev. Lett. **72**, 3112 (1994).
[39] J. Shen, Ph.D. thesis, Martin-Luther University, Halle, Germany, 1996.
[40] J. Giergiel, J. Kirschner, J. Landgraf, J. Shen, and J. Woltersdorf, Surf. Sci. **310**, 1 (1994).
[41] J. Shen, Ch. V. Mohan, P. Ohresser, M. Klaua, and J. Kirschner, Phys. Rev. B **57**, 13 674 (1998).
[42] J. B. Pendry, *Low Energy Electron Diffraction* (Academic, New York, 1974).
[43] See, e.g., *Ultrathin Magnetic Structures I*, edited by J. A. C. Bland and B. Heinrich (Springer-Verlag, Berlin, 1994).
[44] S. Sundar Manoharan, J. Shen, H. Jenniches, M. Klaua, and J. Kirschner, J. Appl. Phys. **81**, 3768 (1997); S. Sundar Manoharan, M. Klaua, J. Shen, J. Barthel, H. Jenniches, and J. Kirschner, Phys. Rev. B **58**, 8549 (1998).
[45] A. Zangwill, in *Evolution of Surface and Thin Film Microstructure*, edited by H. A. Atwater, E. Chason, M. Grabow, and M. Lagally, MRS Symposia Proceedings No. 280 (Materials Re-

search Society, Pittsburgh, 1993), p. 121.
[46] D. D. Chambliss and K. E. Johnson, Phys. Rev. B **50**, 5012 (1994).
[47] C. Ratsch, A. Zangwill, P. Šmilauer, and D. D. Vvedensky, Phys. Rev. Lett. **72**, 3194 (1994).
[48] M. Störmer and H. U. Krebs, J. Appl. Phys. **78**, 7080 (1995).
[49] H. U. Krebs, Int. J. Non-Equilibr. Process. **10**, 3 (1997).
[50] S. Esch, M. Breeman, M. Morgenstern, T. Michely, and G. Comsa, Surf. Sci. **365**, 187 (1996).
[51] W. Wulfhekel, I. Beckmann, N. N. Lipkin, G. Rosenfeld, B. Poelsema, and G. Comsa, Appl. Phys. Lett. **69**, 3492 (1996).
[52] S. Mülle, P. Bayer, A. Kinne, P. Schmailzl, and K. Heinz, Surf. Sci. **322**, 21 (1995).
[53] M. Zharnikov, A. Dittschar, W. Kuch, C. M. Schneider, and J. Kirschner, J. Magn. Magn. Mater. **174**, 40 (1997).
[54] T. Asada and S. Blügel, Phys. Rev. Lett. **79**, 507 (1997).
[55] R. Lorenz and J. Hafner, Phys. Rev. B **54**, 15 937 (1996).
[56] B. Újfalussy, L. Szunyogh, and P. Weinberger, Phys. Rev. B **54**, 9883 (1996).
[57] H. Magnan, D. Chandesris, B. Villette, O. Heckmann, and J. Lecante, Phys. Rev. Lett. **67**, 859 (1991).
[58] D. E. Fowler and J. V. Barth, Phys. Rev. B **53**, 5563 (1996).
[59] D. Spišák and J. Hafner, Phys. Rev. B **56**, 2646 (1997).
[60] P. Bruno, J. Appl. Phys. **64**, 3153 (1988).